The strength of the innate immune response drives the within-host competition between highly and low pathogenic avian influenza viruses

Pierre Bessière[1¶], Thomas Figueroa[1¶], Amelia Coggon[1], Charlotte Foret-Lucas[1], Alexandre Houffschmitt[1], Maxime Fusade-Boyer[1], Gabriel Dupré[1], Maxence Delverdier[1], and Romain Volmer[1*]

[1] Ecole nationale vétérinaire de Toulouse, Université de Toulouse, ENVT, INRAE, IHAP, UMR 1225, Toulouse, France.

* Correspondence:

Dr Romain Volmer

romain.volmer@envt.fr

¶ These authors contributed equally to this work.

ABSTRACT

Highly pathogenic avian influenza viruses (HPAIV) emerge from low pathogenic avian influenza viruses (LPAIV) through the introduction of basic amino acids at the hemagglutinin (HA) cleavage site. Following viral evolution, the newly formed HPAIV likely represents a minority variant within the index host, predominantly infected with the LPAIV precursor. Using reverse-genetics engineered H5N8 viruses differing solely at the HA cleavage, we tested the hypothesis that the interaction between the minority HPAIV and the majority LPAIV could modulate the risk of HPAIV emergence and that the nature of the interaction could depend on the host species. In chickens, we observed that the $H5N8_{LP}$ increased $H5N8_{HP}$ replication and pathogenesis. By contrast, the $H5N8_{LP}$ antagonized $H5N8_{HP}$ replication and pathogenesis in ducks. Ducks mounted a more potent antiviral innate immune response than chickens against the $H5N8_{LP}$, which correlated with $H5N8_{HP}$ inhibition. Our results provide evidence that HPAIV may be more likely to emerge in chickens than in ducks because of differences in the host response to HPAIV and LPAIV co-infections.

35 **INTRODUCTION**

36 Highly pathogenic avian influenza virus (HPAIV) outbreaks have a major
37 impact on animal health, food security and economy, as well as on public
38 health [1,2]. A better understanding of the factors leading to HPAIV
39 emergence is therefore of paramount importance. Avian influenza viruses
40 of H5 and H7 subtypes can become highly pathogenic through the
41 introduction of multiple basic amino acids within the hemagglutinin (HA)
42 cleavage site [3]. Several mechanisms account for these introductions:
43 nucleotide substitutions and insertions or non-homologous recombination
44 with viral or cellular RNAs [1,4,5]. The acquisition of a multi-basic cleavage
45 site (MBCS) is a virus-dependent event that occurs in a bird infected with a
46 parental low pathogenic avian influenza virus (LPAIV). To emerge
47 successfully, the newly formed HPAIV must become a predominant variant
48 in order to overcome the transmission bottleneck between individuals [6–
49 8]. In order to achieve this, the newly formed HPAIV must therefore
50 outcompete its LPAIV precursor within the individual in which it has
51 arisen. We therefore suggest that HPAIV emergence is a two-step process:
52 firstly, the acquisition of a MBCS, followed by the ability to become a
53 predominant variant of the viral quasi-species within an individual.
54 Over the past decades, the vast majority of HPAIV emergences have been
55 linked to H5 and H7 LPAIV circulation in *Galliformes* (such as chickens and
56 turkeys) [1,2,4]. By contrast, *Anseriformes* (such as ducks and geese) are
57 considered as reservoirs for LPAIV precursors, rather than a species in
58 which HPAIV emerge [9–12]. These observations suggest that host factors
59 could modulate HPAIV emergence. To our knowledge, this has never been
60 investigated experimentally.

61 To model the intra-host competition between a newly formed HPAIV and
62 its parental LPAIV, we co-infected embryonated eggs and chickens and
63 ducks *in vivo* with a H5N8 HPAIV as a minority variant and a reverse-
64 genetics engineered LPAIV that differed from the HPAIV only at the level of
65 the HA cleavage site, as a majority variant. Our results demonstrate that
66 chickens and ducks have opposite effects on the interaction between the

67 H5N8 HPAIV and LPAIV and that the HPAIV has a stronger selective
68 advantage in chickens than in ducks. To our knowledge this is the first
69 experimental evidence that HPAIV emergence could be more likely in
70 chickens than in ducks.

71

72 **RESULTS**

73 **Characterization of $H5N8_{HP}$ and $H5N8_{LP}$ viruses in cell culture**

74 We used reverse-genetics to generate the wild-type $H5N8_{HP}$ from a HPAIV
75 isolated during the 2016 H5N8 epizootics in France [13]. This virus
76 belonged to clade 2.3.4.4 group B, which caused high levels of mortality in
77 *Galliformes* and in wild and domestic *Anseriformes* during the 2016-2017
78 HPAIV outbreak in Europe [13–16]. Using site-directed mutagenesis and
79 reverse-genetics, we mutated the $H5N8_{HP}$ HA polybasic cleavage site
80 PLRELRRLR/G to a monobasic cleavage site PQRETR/G to obtain the
81 $H5N8_{LP}$ virus with a typical LPAIV HA sequence (NCBI Genbank accession
82 number: AB261853.1) [17]. The $H5N8_{HP}$ and the $H5N8_{LP}$ differed solely at
83 the level of the HA cleavage site, as verified by whole genome sequencing
84 following virus amplification in chicken embryonated eggs (Fig. 1A).
85 Viral growth kinetics was analyzed in Madin-Darby canine kidney (MDCK)
86 cells, in the DF-1 chicken fibroblast cell line and in the CCL-141 duck
87 fibroblast cell line infected at a multiplicity of infection (MOI) of 10^{-5} tissue
88 culture infectious dose 50 ($TCID_{50}$). $H5N8_{HP}$ replicated with similar kinetics
89 in the absence or presence of exogenous trypsin, demonstrating that
90 proteolytic processing of the HA MBCS was independent of trypsin-like
91 proteases, as expected for a HPAIV (Fig. 1B). By contrast, $H5N8_{LP}$
92 replication was severely impaired in the absence of trypsin, while its
93 replication kinetics was indistinguishable from that of the $H5N8_{HP}$ in the
94 presence of trypsin (Fig. 1B). These results indicate that mutations
95 introduced in the $H5N8_{LP}$ HA have no negative impact on viral replication
96 kinetics in cell culture beyond the expected trypsin-like proteases
97 requirement for $H5N8_{LP}$ HA proteolytic processing, as expected for a LPAIV.
98

99 **$H5N8_{HP}$ and $H5N8_{LP}$ viruses co-infections *in ovo***

100 Next, we evaluated $H5N8_{HP}$ and $H5N8_{LP}$ replication in embryonated chicken
101 (*Gallus gallus*) and Pekin duck (*Anas platyrhynchos domesticus*) eggs, as
102 they have a complex cellular architecture and provide an intermediate
103 model between monolayer cell culture and *in vivo* studies. To investigate
104 how the host species modulated the interaction between a HPAIV and a
105 LPAIV, we inoculated embryonated chicken and duck eggs via the allantoic
106 cavity either with 10^2 egg infectious dose 50 (EID_{50}) $H5N8_{HP}$ alone, with
107 increasing doses of $H5N8_{LP}$ alone, or with 10^2 EID_{50} $H5N8_{HP}$ in combination
108 with increasing doses of $H5N8_{LP}$ (Fig. 2A). We inoculated chicken eggs at
109 day 10 and duck eggs at day 11 in order to work at similar development
110 stages [18]. After 24 hours of incubation at 37°C, we harvested the allantoic
111 fluid and quantified the level of virus replication by RT-qPCR using primers
112 specific for $H5N8_{HP}$ or $H5N8_{LP}$ HA. In chicken eggs, we detected equivalent
113 levels of viral RNA following inoculation with 10^2EID_{50} $H5N8_{HP}$ alone or
114 with $H5N8_{LP}$ alone regardless of the inoculum dose (Fig. 2B). Upon co-
115 infection with $H5N8_{HP}$ and $H5N8_{LP}$ in chicken eggs, the level of $H5N8_{HP}$ and
116 $H5N8_{LP}$-specific viral RNA did not differ from mono-infections regardless of
117 the quantity of $H5N8_{LP}$ (Fig. 2B). Thus, the replication of $H5N8_{HP}$ is not
118 affected by $H5N8_{LP}$, regardless of the amount of $H5N8_{LP}$ co-inoculated in
119 chicken eggs. In duck eggs, we detected similar levels of viral RNA following
120 inoculation with 10^2 EID_{50} $H5N8_{HP}$ alone or with 10^2 EID_{50} $H5N8_{LP}$ alone
121 (Fig. 2C). When duck eggs were infected simultaneously with $H5N8_{HP}$ and
122 $H5N8_{LP}$, we observed a decrease of $H5N8_{HP}$ viral RNA levels that correlated
123 with the amount of $H5N8_{LP}$ co-inoculated, indicating that the $H5N8_{LP}$
124 antagonized $H5N8_{HP}$ replication in duck eggs (Fig. 2C). The *in ovo*
125 experiments provide evidence that a ≥100-fold excess of $H5N8_{LP}$
126 significantly antagonized $H5N8_{HP}$ replication in duck eggs, while $H5N8_{LP}$
127 did not affect $H5N8_{HP}$ replication in chicken eggs regardless of the amount
128 of $H5N8_{LP}$. This observation thus indicates that the $H5N8_{HP}$ had a stronger
129 selective advantage over the $H5N8_{LP}$ in chicken embryonated eggs than in
130 duck embryonated eggs.
131

132 **Potentiation of HPAIV replication and pathogenesis by LPAIV in**
133 **chickens**

134 In a preliminary experiment (data not shown), we observed transient low-
135 level oropharyngeal viral RNA shedding in 6/8 of the 10^6 EID_{50} $H5N8_{LP}$
136 infected chickens (*Gallus gallus*), whereas all chickens infected with 10^7
137 EID_{50} $H5N8_{LP}$ shed high levels of viral RNA for a prolonged time. No clinical
138 signs were observed in chickens inoculated with $H5N8_{LP}$. We evaluated the
139 $H5N8_{HP}$ chicken infectious dose 50 at $6x10^3$ EID_{50}. $H5N8_{HP}$-infected sick
140 birds presented dyspnea that quickly progressed to severe dyspnea,
141 associated with anorexia and lethargy. These results provided evidence
142 that the $H5N8_{HP}$ and $H5N8_{LP}$ caused, respectively, commonly observed
143 HPAIV and LPAIV-associated infection patterns in chickens [2].
144 Based on these results, we investigated the interaction between a HPAIV
145 and a LPAIV in chickens. Four-week old chickens were assigned one of six
146 groups: L7, H3, H4, L7H3, L7H4 or NI (Fig. 3A). L7 animals were infected
147 with 10^7 EID_{50} $H5N8_{LP}$. H3 animals were infected with 10^3 EID_{50} $H5N8_{HP}$.
148 H4 animals were infected with 10^4 EID_{50} $H5N8_{HP}$. L7H3 animals were
149 infected with a mixture of 10^7 EID_{50} $H5N8_{LP}$ and 10^3 EID_{50} $H5N8_{HP}$. L7H4
150 animals were infected with a mixture of 10^7 EID_{50} $H5N8_{LP}$ and 10^4 EID_{50}
151 $H5N8_{HP}$. Finally, non-infected animals from group NI were administered
152 vehicle only. Neither mortality nor clinical signs were observed in chickens
153 from group L7 and group H3 (Fig. 3B). Chickens in the H4 group reached
154 45% mortality (Fig. 3B). When chickens were infected with a mixture of
155 $H5N8_{LP}$ and $H5N8_{HP}$, we observed an increase in mortality compared to
156 $H5N8_{HP}$ mono-infected chickens: mortality reached 18% in the L7H3 group,
157 compared to 0% in the H3 group; and 72% in the L7H4 group, compared to
158 45% in the H4 group (Fig. 3B). Although the increase in mortality did not
159 reach statistical significance, these results indicate that $H5N8_{LP}$ and $H5N8_{HP}$
160 synergized, resulting in increased pathogenesis in co-infected chickens
161 compared to $H5N8_{HP}$ mono-infected chickens.
162 We measured viral shedding from oropharyngeal and cloacal swabs by
163 quantifying viral RNA using RT-qPCR with primers detecting specifically
164 $H5N8_{LP}$ or $H5N8_{HP}$ HA sequences. Regardless of the experimental group, all

165 $H5N8_{HP}$ swab-positive chickens eventually developed severe dyspnea and
166 either died or were euthanized when they reached humane endpoints, as
167 previously observed [19]. In line with the mortality rate (Fig 3B), no
168 $H5N8_{HP}$ swab-positive chicken was found in the H3 group, while only two
169 chickens tested positive for $H5N8_{HP}$ in the L7H3 group. Because of the low
170 rate of infection in the H3 and L7H3 groups, these animals were excluded
171 from further analyses. $H5N8_{HP}$ oropharyngeal and cloacal shedding was
172 higher in group L7H4 compared to group H4 at 2 days post-infection (dpi),
173 but the difference was not statistically significant (Fig. 3C&D). Average
174 $H5N8_{HP}$ oropharyngeal and cloacal shedding remained otherwise similar
175 between the L7H4 and the H4 groups and was not associated with different
176 $H5N8_{HP}$ transmission rates to contact chickens introduced in the poultry
177 isolators at 1 dpi (data not shown). $H5N8_{LP}$ oropharyngeal shedding did not
178 differ between the L7 and L7H4 group (Fig. 3E).
179 $H5N8_{LP}$ RNA was not detected from the lungs or brain of any animal,
180 indicating that $H5N8_{LP}$ replicated mostly in the upper respiratory tract of
181 chickens. $H5N8_{HP}$ viral RNA was detected at similar levels in the lungs and
182 brain of moribund animals from groups L7H4 and H4 that were euthanized,
183 but was not detected in the lungs and brain from animals autopsied at 1
184 and 3 dpi (Fig. 3F&G). These results indicate that $H5N8_{HP}$ replicated in the
185 upper respiratory tract in the early stages of infection (*i.e.* until 3 dpi). In
186 line with the predominantly respiratory clinical signs observed in
187 moribund animals, moderate viral antigen staining was detected by
188 immunohistochemistry in the brain, while extensive viral antigen staining
189 was detected in the lungs (Fig. 4).
190 We next evaluated the expression of host immune response markers using
191 RT-qPCR. We observed a modest but significant upregulation of Mx and
192 interferon gamma (IFN-γ) mRNA expression only in the lungs of moribund
193 chickens (Fig. 5A&B). Mx is a type I IFN-induced gene whose expression is a
194 good indicator of the amount of type I IFN active locally [20]. The lack of
195 changes in Mx and IFN-γ mRNA expression in the lungs of animals at 1 and
196 3 dpi was probably related to the fact that no viral RNA could be detected in
197 the lungs of these animals (Fig. 5A). Since oropharyngeal swabs were

198 mostly positive for viral RNA at any time post-infection, we analyzed the
199 antiviral innate immune response in the upper respiratory tract by
200 measuring Mx mRNA expression by RT-qPCR from RNA extracted from
201 oropharyngeal swabs (Fig. 5C). Compared to NI animals, Mx mRNA was
202 significantly increased in groups L7H4 and L7 at 1 dpi. At 2 and 3 dpi, Mx
203 mRNA was significantly increased in groups L7H4 and H4. Interestingly, in
204 group L7, Mx mRNA levels decreased rapidly and were not significantly
205 different from NI chickens from 2 dpi onwards, indicating that $H5N8_{LP}$
206 mono-infected chickens had a transient upregulation of Mx mRNA
207 expression in the upper respiratory tract. Altogether, these results indicate
208 that the chicken immune response to viral infection was modest and
209 transient. In addition, the chicken immune response did not differ between
210 $H5N8_{HP}$ mono-infected birds (group H4) and $H5N8_{LP}$ and $H5N8_{HP}$ co-
211 infected birds (group L7H4).
212 To gain insight into the reasons underlying the difference in mortality
213 between H4 and L7H4, we plotted individual $H5N8_{HP}$ oropharyngeal
214 shedding curves from the onset of excretion to the death of the animal (Fig.
215 6A). We observed that the slopes of $H5N8_{HP}$ excretion were significantly
216 steeper in the L7H4 group than in the H4 group, suggesting that the rate of
217 $H5N8_{HP}$ growth was higher (Fig. 6B). In complement to this observation, we
218 noticed that all $H5N8_{LP}$ and $H5N8_{HP}$ co-infected birds in the L7H4 group
219 died within 48 hours following the first $H5N8_{HP}$ positive swab (Fig. 6C). By
220 contrast, $H5N8_{HP}$ was shed significantly longer in $H5N8_{HP}$ mono-infected
221 birds from the H4 group (Fig. 6C). Thus, analysis of individual
222 oropharyngeal excretion patterns revealed that $H5N8_{HP}$ growth rate was
223 higher when animals were co-infected with $H5N8_{LP}$, compared to $H5N8_{HP}$
224 mono-infected chickens. In conclusion, these results show that there was
225 synergy between $H5N8_{LP}$ and $H5N8_{HP}$ in co-infected chickens, resulting in
226 increased $H5N8_{HP}$ growth and pathogenesis compared to $H5N8_{HP}$ mono-
227 infected chickens.
228
229
230

231 **Antagonism of HPAIV replication and pathogenesis by LPAIV in ducks**

232 We inoculated groups of 4-week old Pekin ducks (*Anas platyrhynchos*
233 *domesticus*) with $H5N8_{HP}$ alone, $H5N8_{LP}$ alone, or a mixture containing both
234 $H5N8_{LP}$ and $H5N8_{HP}$. Ducks were assigned one of four groups: L7, H4, L7H4
235 or NI (Fig. 7A). L7 animals were infected with 10^7 EID_{50} $H5N8_{LP}$. H4 animals
236 were infected with 10^4 EID_{50} $H5N8_{HP}$. L7H4 animals were infected with a
237 mixture of 10^7 EID_{50} $H5N8_{LP}$ and 10^4 EID_{50} $H5N8_{HP}$. Non-infected animals
238 from group NI were administered vehicle only. Neither mortality nor
239 clinical signs were observed in any duck of group L7 (Fig. 7B). Mortality
240 reached 87% in the H4 group and was preceded by predominantly
241 neurological clinical signs, in accordance with the pronounced
242 neurotropism of clade 2.3.4.4 group B H5N8 viruses in ducks [14–16].
243 Mortality was significantly reduced to 37% in the L7H4 group. Thus,
244 $H5N8_{LP}$ antagonized $H5N8_{HP}$ pathogenesis in co-infected ducks, in contrast
245 to what we observed in chickens.
246 To determine how this related to the levels of virus replication, we
247 analyzed $H5N8_{LP}$ and $H5N8_{HP}$ viral RNA shedding from oropharyngeal and
248 cloacal swabs using RT-qPCR. Oropharyngeal $H5N8_{HP}$ shedding was
249 significantly reduced in group L7H4 compared to group H4 in the first days
250 post-infection (dpi), with a hundred-fold difference at 1 dpi ($p<0.001$) and
251 a ten-fold difference at 2 and 3 dpi ($p<0.01$) (Fig. 7C). Cloacal $H5N8_{HP}$
252 shedding was also decreased in group L7H4, but the difference only
253 reached statistical difference at day 3, with a ten-fold reduction ($p<0.05$)
254 (Fig. 7D). There was no difference in $H5N8_{LP}$ shedding between groups
255 L7H4 and L7 (Fig. 7E).
256 Next, we analyzed viral RNA levels in the lungs and brain. $H5N8_{LP}$ was not
257 detected in the lungs or brain, indicating that $H5N8_{LP}$ replicated mostly in
258 the upper respiratory tract of ducks. In contrast to chickens, we detected
259 $H5N8_{HP}$ nucleic viral RNA from the lungs and brain of most animals at 1 and
260 3 dpi (Fig. 7F&G). $H5N8_{HP}$ viral RNA load was decreased in the lungs and
261 brain of $H5N8_{LP}$ and $H5N8_{HP}$ co-infected birds (group L7H4), compared to
262 $H5N8_{HP}$ mono-infected birds (group H4). High levels of $H5N8_{HP}$ viral RNA
263 were also detected in the lungs and brain of moribund ducks, which

264 developed predominantly neurological signs. Extensive viral antigen
265 staining was detected by immunohistochemistry in the brain of moribund
266 animals, while more modest viral antigen staining was observed in the
267 lungs, with no difference between groups L7H4 and H4 (Fig. 8A&B).
268 We then evaluated the expression of host immune response markers in the
269 lungs and brain using RT-qPCR. Mx mRNA expression was significantly
270 increased in the lungs of infected ducks belonging to the L7H4 and H4
271 groups at 1 and 3 dpi, as well as in moribund animals (Fig. 9A). Compared
272 to NI duck, we also observed an upregulation of Mx mRNA expression in
273 the lungs of $H5N8_{LP}$ mono-infected ducks (L7 group) at 1 and 3 dpi,
274 although the difference did not reach statistical significance. IFN-γ mRNAs
275 levels were significantly higher in the lungs of $H5N8_{HP}$ mono-infected ducks
276 (group H4) at 1 dpi compared to NI, L7H4 and L7 ducks (Fig. 9B). Similar
277 results were observed in the brain (data not shown). To evaluate the
278 antiviral innate immune response in the upper respiratory tract, we
279 measured Mx mRNA expression by RT-qPCR from RNA extracted from
280 oropharyngeal swabs. Compared to NI ducks, Mx mRNA was increased in
281 all infected groups (Fig. 9C). In contrast to chickens, Mx mRNA expression
282 level remained high in $H5N8_{LP}$ mono-infected ducks from the L7 group (Fig.
283 9C).

284 To further compare the antiviral innate immune response in ducks and
285 chickens, we plotted the levels of Mx mRNA as a function of the level of viral
286 RNA in the lungs (Fig. 10A). We observed a correlation between the level of
287 Mx mRNA and the level of viral RNA in ducks (Pearson $r=0.64$; $p<0.001$),
288 confirming that the intensity of the antiviral innate immune response is
289 proportional to the level of viral RNA, as previously reported [21–24]. This
290 correlation was less visible in chickens, possibly because viral RNA was
291 only found in the lungs of a limited number of chickens (Pearson $r=0.50$;
292 $p=0.21$). The Mx/HA ratios were distributed to higher values in ducks
293 compared to chickens (Fig. 10A), resulting in mean Mx/HA ratios that were
294 significantly higher in ducks than in chickens (Fig. 10B). This result
295 demonstrates that ducks mounted a more potent antiviral innate immune
296 response against influenza virus infection than chickens.

297 **DISCUSSION**

298 To model the intra-host competition between a newly formed HPAIV and
299 its parental LPAIV, we inoculated chickens and ducks with an $H5N8_{HP}$ virus
300 and an $H5N8_{LP}$ virus differing solely at the level of the HA cleavage site.
301 When inoculated alone, $H5N8_{HP}$ replication and pathogenesis were
302 equivalent in chickens and ducks. However, when chickens and ducks were
303 co-inoculated with this pair of viruses, we found that the $H5N8_{HP}$ had a
304 stronger selective advantage over the $H5N8_{LP}$ in chickens than in ducks.
305 Surprisingly, we observed that the $H5N8_{LP}$ increased $H5N8_{HP}$ replication
306 and pathogenesis in chickens. By contrast, we observed that the $H5N8_{LP}$
307 antagonized $H5N8_{HP}$ replication and pathogenesis in ducks. Thus, the
308 nature of the interaction between the HPAIV and the parental LPAIV may
309 be a critical determinant of HPAIV emergence, which we show here to
310 depend on the host species.

311 The interaction between co-infecting viruses ranges from synergy to
312 antagonism depending on the virus pairs and the host [25–31]. Functional
313 complementation occurs when one virus provides a function that is absent
314 or less efficient in the other virus. As the genomes of the $H5N8_{HP}$ and
315 $H5N8_{LP}$ differ solely at the level of the HA cleavage site, it is unlikely that
316 the $H5N8_{LP}$ is able to provide a function missing in the $H5N8_{HP}$. We
317 therefore speculate that the $H5N8_{LP}$-mediated increase in $H5N8_{HP}$
318 replication and pathogenesis observed in chickens could be due to
319 complementation of semi-infectious $H5N8_{HP}$ particles by the $H5N8_{LP}$
320 inoculated at a higher dosage [32]. Such complementation is likely to occur
321 both in chickens and in ducks. However, this complementation may be
322 undetectable in ducks due to the dominant effect of host-mediated
323 antagonism between the $H5N8_{LP}$ and the $H5N8_{HP}$. The antagonism between
324 the $H5N8_{LP}$ and the $H5N8_{HP}$ is unlikely to be due to viral interference due to
325 receptor or cell machinery usage, as no competition between the $H5N8_{LP}$
326 and the $H5N8_{HP}$ was observed in chickens, although the $H5N8_{LP}$ replicated
327 to higher levels and persisted longer in chickens than in ducks. Our results
328 suggest that the competition between the $H5N8_{LP}$ and the $H5N8_{HP}$ was only

329 observed in ducks because ducks mounted a more pronounced antiviral
330 innate immune response than chickens against the $H5N8_{LP}$. Indeed, in
331 contrast to chickens, ducks have a functional RIG-I receptor, which has
332 been proposed to contribute to the more efficient type I interferon
333 mediated-antiviral innate immune response against influenza viruses
334 observed in ducks compared to chickens [22,33–38]. The $H5N8_{LP}$ and the
335 $H5N8_{HP}$ are likely to be intrinsically equally sensitive to the antiviral effects
336 of type I interferon. However, a stronger antiviral innate immune response
337 could impose a stronger selective pressure on the minority variant [39]. In
338 line with this hypothesis, type I interferon antiviral innate immune
339 response was shown to constitute a strong bottleneck shaping poliovirus
340 population in mice [40]. We therefore suggest that the more pronounced
341 antiviral innate immune response observed in ducks compared to chickens
342 imposed a stronger selective pressure on the $H5N8_{HP}$ minority variant,
343 compared to the $H5N8_{LP}$ inoculated at a higher dosage. The antiviral innate
344 immune response may thus inhibit the selection of variants that arise
345 through *de novo* mutations during infection of an individual, unless these
346 variants have a strong selective advantage within this individual.

347 Recent work investigating the interaction between an H7N7 HPAIV and a
348 closely related H7N7 LPAIV field isolate demonstrated that the LPAIV
349 inhibited HPAIV replication in chickens when the LPAIV was inoculated at a
350 ≥ 100-fold higher dose [41]. These results indicate that the nature of the
351 interaction between the HPAIV and the LPAIV may depend on the viral
352 strain. If competition between a LPAIV and a HPAIV occurred in chickens,
353 we speculate that the competition could even be stronger in ducks, because
354 of the stronger antiviral innate immune-mediated selective pressure
355 imposed on the minority HPAIV. However, further work is needed to
356 properly address this question. These studies should ideally be performed
357 using different pairs of reverse-genetics engineered HPAIV and LPAIV
358 differing solely at the level of the HA cleavage site to specifically investigate
359 how the selective advantage conferred by the MBCS depends on the host
360 species.

361 Epidemiological investigations of HPAIV outbreaks indicate that the vast
362 majority of HPAIV emerge upon replication and inter-individual
363 transmission of a LPAIV in *Galliformes*, such as chickens and turkeys,
364 although *Anseriformes*, such as ducks and geese, are considered as the main
365 reservoirs for LPAIV [1,2,4,5]. In this study, we focused on the two main
366 representatives of the *Galliformes* and *Anseriformes* orders: chickens, which
367 are with current global production of 22 billion chickens the main source of
368 animal protein for human consumption worldwide and Pekin ducks, which
369 are also intensively raised in farms and represent the best characterized
370 *Anseriformes* in respect to the interaction with influenza viruses [1,42]. Our
371 results suggest that HPAIV would be more likely to emerge in chickens than
372 in ducks because of differences in their response to influenza virus
373 infection. How the host response could influence the interaction between
374 the LPAIV and the newly formed HPAIV in other bird species, such as
375 turkeys, or in wild dabbling or diving ducks, which have a prominent role in
376 the ecology of avian influenza viruses will be the subject of future studies
377 [1,2,9]. In addition to host factors, anthropic factors are also likely to play a
378 major role in the emergence of HPAIV and may contribute to the higher
379 frequency of HPAIV emergence observed in chickens that are usually raised
380 at higher densities than ducks [5,43–45]. Estimating to which extent
381 farming processes contribute to the emergence of HPAIV is however a
382 difficult task and therefore their contribution to HPAIV emergence remains
383 currently unclear.

384 To minimize the risk of HPAIV evolution, present European regulation and
385 national regulations in many countries require the culling of all birds in
386 flocks infected with H5 and H7 LPAIV [2]. Culling of H5 or H7 LPAIV
387 infected flocks aims at eliminating LPAIV from the susceptible poultry
388 population before they have a chance to evolve into HPAIV, and is therefore
389 considered a preventive biosecurity measure. However, the broader public,
390 breeders and professional breeder societies question the need for
391 preventive culling for economical, animal welfare and breeder welfare
392 issues [46]. Indeed, preventive culling of animals, especially healthy
393 animals, which is commonly the case in LPAIV infected *Anseriformes*, is

394 poorly accepted. Identifying how host factors modulate HPAIV emergence
395 therefore provides important scientific data that may be taken into account
396 by animal health policy makers in the future.

397 ## MATERIALS AND METHODS

398 ### Ethics statement

399 This study was carried out in compliance with European animal welfare
400 regulation. The protocols were approved by the Animal Care and Use
401 Committee (Comité d'Ethique en Science et Santés Animales – 115) under
402 protocol 13025-2018012311319709.

403

404 ### Viruses

405 The eight segments from the HPAIV field isolate A/mulard
406 duck/France/171201g/2017 (H5N8) were cloned in a pHW2000 plasmid
407 vector using a set of universal primers in order to generate a reverse-
408 genetics engineered wild-type HPAIV H5N8 ($H5N8_{HP}$) [47,48]. Using site-
409 directed mutagenesis, a 9 nucleotides deletion was performed on the HA
410 cleavage site sequence, along with two single nucleotide polymorphism on
411 both sides of the deletion to obtain a reverse-genetics engineered LPAIV
412 H5N8 ($H5N8_{LP}$) according to the manufacturer's instructions (In-Fusion,
413 Takara Bio, France). $2.5x10^5$ HEK 293T cells cultured in 6-well plates were
414 transfected in Opti-MEM medium, using the lipophilic transfection reagent
415 LTX with Plus reagent (Invitrogen, Thermo Fisher Scientific Inc., Canada),
416 either with 0.5µg of each seven common $H5N8_{HP/LP}$ pHW2000 plasmids
417 (PB2, PB1, PA, NA, NP, M and NS) and with 0.5µg of HA_{HP} or HA_{LP}. L-
418 (tosylamido-2-phenyl)ethyl chloromethyl ketone (TPCK) treated trypsin
419 (TPCK-treated) was added 24 hours post-transfection at a 0.5µg/ml final
420 concentration. 48 hours post-transfection, scraped cells and culture
421 medium were transferred on MDCK cells grown with Opti-MEM
422 supplemented with 0.5µg/ml TPCK-treated trypsin. 72 hours later, cell
423 supernatant was collected. To produce viral stock, both viruses were then
424 propagated in 10-day-old chicken specific-pathogen-free (SPF)
425 embryonated chicken eggs (INRAE, PFIE, Nouzilly, France), by inoculation
426 in the allantoic cavity of 100µL of 1:100 dilutions of infected MDCK cells
427 supernatant. Infectious allantoic fluid was harvested at 72 hours
428 postinoculation and titrated in 10-day-old SPF embryonated chicken eggs
429 to determine the 50% egg infective dose (EID_{50})/mL using the Reed-

430 Muench method. The identity of amplified viruses was verified by Sanger
431 sequencing of each viral gene segment ($H5N8_{HP}$: accession numbers
432 MK859904 to MK859911; $H5N8_{LP}$: accession numbers MK859926 to
433 MK859933). These viruses were referenced by the French biotechnology
434 ethics committee (Haut Conseil des Biotechnologies) and were manipulated
435 exclusively in biosafety level 3 laboratories.
436
437 ***In vitro* infections**
438 MDCK cells, DF-1 cells and CCL-141 cells were cultured in DMEM
439 containing 1% antibiotics (penicillin/streptomycin) and 10% fetal bovine
440 serum. When cells reach 90% confluency, they were washed with PBS and
441 infected either with $H5N8_{HP}$ or with $H5N8_{LP}$ at a multiplicity of infection
442 (MOI) of 10^{-5} $TCID_{50}$. After one hour, the inoculum was removed, cells were
443 washed twice with PBS and Opti-MEM supplemented with 0.5µg/mL TPCK-
444 treated trypsin (Pierce, Thermo Fisher Scientific Inc., Canada) was added.
445 Viral RNA extraction was performed on 140µL supernatant collected at 1,
446 24, 48 and 72 hours post-infection according to the manufacturer's
447 instructions (QIAamp viral RNA; Qiagen, Toronto, Canada). Influenza
448 nucleic acid load was determined by RT-qPCR using primers targeting both
449 $H5N8_{LP}$ and $H5N8_{HP}$ HA gene in a final volume of 10µL. Mixes were
450 prepared according to the manufacturer's instructions (iTaq Universal
451 SYBR green One-Step kit, BioRad) with 1µL of RNA and a final
452 concentration of 0.3µM of each primer.
453
454 ***In ovo* co-infection experiments**
455 Specific pathogen-free (SPF) White Leghorn (PA12) embryonated chicken
456 eggs (PFIE, INRAE, Nouzilly, France) and Pekin Duck (ST5 Heavy)
457 embryonated eggs (ORVIA-Couvoir de la Seigneurtière, Vieillevigne,
458 France) were respectively incubated for 10 and 11 days at 37°C to work at
459 similar stages of development [18]. They were then inoculated in the
460 allantoic cavity with 200µL virus diluted in PBS containing 1% antibiotics
461 (penicillin/streptomycin). Eggs from group H2 were infected with 10^2
462 EID_{50} $H5N8_{HP}$. Eggs from groups L2, L3, L4 and L5 were infected with 10^2

463 EID_{50}, 10^3 EID_{50}, 10^4 EID_{50}, and 10^5 EID_{50} $H5N8_{LP}$ respectively. Eggs from
464 groups L2H2, L3H2, L4H2 and L5H2 were infected with a mixture of 10^2
465 EID_{50} $H5N8_{HP}$ and increasing doses of $H5N8_{LP}$: 10^2, 10^3, 10^4 and 10^5 EID_{50}
466 $H5N8_{LP}$ respectively. Each group contained 9 to 29 eggs from two to three
467 independent experiments. 24 hours post-infection eggs were incubated at
468 4°C overnight and allantoic fluid was harvested for RNA extraction.

469

470 **Animals and groups**

471 Chickens and ducks experiment were conducted separately. One-day-old
472 Pekin ducklings (*Anas platyrhyncos domesticus*, ST5 heavy) were obtained
473 from a commercial hatchery (ORVIA-Couvoir de la Seigneurtière,
474 Vieillevigne, France) and one-day-old White Leghorn chicks (*Gallus gallus*
475 *domesticus*, PA12) from a research hatchery (PFIE, INRAE, Nouzilly,
476 France). Animals were fed *ad libitum* with a starter diet and housed in
477 biosafety level II facilities for 2 weeks in a litter-covered floor pen at the
478 National Veterinary School of Toulouse, France. They were then transferred
479 into a biosafety level III facility, equipped with bird isolators (I-Box; Noroit,
480 Nantes, France) ventilated under negative pressure with HEPA-filtered air.
481 Chicken preliminary experiment: 39 chickens were randomly assigned to
482 four groups: 10 animals were assigned to group H3 and were infected with
483 10^3 EID_{50} $H5N8_{HP}$. 10 animals were assigned to group H4 and were infected
484 with 10^4 EID_{50} $H5N8_{HP}$. 8 animals were assigned to group L6 and were
485 infected with 10^6 EID_{50} $H5N8_{LP}$. 11 animals were assigned to group L7 and
486 were infected with 10^7 EID_{50} $H5N8_{LP}$.
487 Chickens co-infection experiment: A total of 130 chickens were randomly
488 assigned to 4 groups: 26 animals (including 5 contact birds introduced 24
489 hours post-infection) were assigned to group H3 and were infected with
490 10^3 EID_{50} $H5N8_{HP}$. 26 animals (including 5 contact birds) were assigned to
491 group H4 and were infected with 10^4 EID_{50} $H5N8_{HP}$. 21 animals were
492 assigned to group L7 and were infected with 10^7 EID_{50} $H5N8_{LP}$. 26 animals
493 (including 5 contact birds) were assigned to group L7H3 and were
494 simultaneously infected with a mixture of 10^7 EID_{50} $H5N8_{LP}$ and 10^3 EID_{50}
495 $H5N8_{HP}$. 26 animals (including 5 contact birds) were assigned to group

496 L7H4 and were simultaneously infected with a mixture of 10^7 EID_{50} $H5N8_{LP}$
497 and 10^4 EID_{50} $H5N8_{HP}$. 5 animals were assigned to the non-infected control
498 group (NI).
499 Ducks co-infection experiment: A total of 64 ducks were randomly assigned
500 to 4 groups: 21 animals (including 3 contact birds) were assigned to group
501 H4 and were infected with 10^4 EID_{50} $H5N8_{HP}$. 16 animals were assigned to
502 group L7 and were infected with 10^7 EID_{50} $H5N8_{LP}$. 21 animals (including 3
503 contact birds) were assigned to group L7H4 and were simultaneously
504 infected with a mixture of 10^7 EID_{50} $H5N8_{LP}$ and 10^4 EID_{50} $H5N8_{HP}$. 5
505 animals were assigned to the non-infected control group (NI).
506
507 ***In vivo* experimental infections**
508 Serum was collected from all animals pre-infection to ensure that they
509 were serologically negative to influenza virus by using a commercial
510 influenza A NP antibody competition enzyme-linked immunosorbent assay
511 kit (ID Screen; ID-Vet, Montpellier, France) according to the manufacturer's
512 instructions. When they were 4-week-old, animals were infected through
513 the choanal route using an inoculum volume of 100µL. Non-infected groups
514 received the equivalent volume of allantoic fluid collected from non-
515 infected SPF embryonated chicken eggs. Contact birds were introduced in
516 the poultry isolators 1 day post-infection. Clinical signs were recorded over
517 8 to 9 days. Oropharyngeal and cloacal swabs were performed on all
518 animals daily. 5 animals from each group were humanely euthanized and
519 necropsied at 1 and 3 dpi. Moribund animals reaching humane termination
520 criteria (as dyspnea, convulsions, severe lethargy) were humanely killed
521 and also necropsied. For each necropsied animal, brain and lungs were
522 collected and stored frozen in TRIzol reagent (Invitrogen, Carlsbad, CA) or
523 stored in 10% neutral formalin.
524
525 **$H5N8_{LP}$ and $H5N8_{HP}$ quantification**
526 Cloacal and oropharyngeal swabs from *in vivo* experiments were briefly
527 vortexed in 500µL of sterile PBS and viral RNA was extracted from 200µL
528 using a QiaCube automated platform according to the manufacturer's

529 instructions (Cador Pathogen QIAcube HT kit; Qiagen, Toronto, Canada).
530 Allantoic fluids from *in ovo* experiments were collected and viral RNA was
531 extracted from 140µL according to the manufacturer's instructions
532 (QIAamp viral RNA; Qiagen, Toronto, Canada). cDNA was synthesized by
533 reverse transcription of 5µL of RNA, using a HA-specific primer (5'-
534 GTCCTTGCGACTG-3') and a RevertAid first-strand cDNA synthesis kit
535 (Invitrogen, Thermo Fisher Scientific) according to the manufacturer's
536 instructions. Influenza nucleic acid load was determined by qPCR using
537 primers targeting either the polybasic or the monobasic HA cleavage site.
538 qPCR was performed in 384-well plates in a final volume of 10µL using a
539 Bravo automated liquid handling platform (Agilent Technologies, Palo Alto,
540 CA) and a ViaaA 7 real-time PCR system (Applied Biosystems, Foster City,
541 CA) at the GeT-TRiX platform (GénoToul, Génopole, Toulouse, France).
542 Mixes were prepared according to the manufacturer's instructions (iTaq
543 SYBR green PCR, BioRad) with 2µL of cDNA and a final concentration of
544 0.5µM of each primer. Absolute quantification was performed using a
545 standard curve based on 10-fold serial dilutions of plasmid containing
546 either $H5N8_{LP}$ or $H5N8_{HP}$ HA gene.
547
548 **RNA extraction from tissue samples and cDNA synthesis**
549 For each organ, 30mg portions of tissue were placed in tubes with beads
550 (Precellys lysis kit; Stretton Scientific, Ltd., Stretton, United Kingdom) filled
551 with 1mL of TRIzol reagent (Invitrogen, Carlsbad, CA) and mixed for 5s at
552 6,000rpm three times in a bead beater (Precellys 24; Bertin Technologies,
553 Montigny-le-Bretonneux, France). After TRIzol extraction, the aqueous
554 phase was transferred to a RNA extraction column and processed according
555 to the manufacturer's instructions (NucleoSpin RNA; Macherey-Nagel
556 GmbH & Co, Germany). cDNA was synthesized by reverse transcription of
557 500ng of total RNA using either both oligo(dT)18 (0.25µg) and random
558 hexamer (0.1µg) primers or HA-specific primer and a RevertAid first-
559 strand cDNA synthesis kit (Invitrogen, Thermo Fisher Scientific) according
560 to the manufacturer's instructions.
561

562 **Quantitative PCR from tissue samples**

563 Quantitative PCR for the analysis of host genes expression was performed
564 in 384-well plates in a final volume of 10µL using a Bravo automated liquid
565 handling platform (Agilent Technologies, Palo Alto, CA) and a ViiA 7 real-
566 time PCR system (Applied Biosystems, Foster City, CA) at the GeT-TRiX
567 platform (GenoToul, Genopole, Toulouse, France). Mixes were prepared
568 according to the manufacturer's instructions (iTaq SYBR green PCR,
569 BioRad) with 2µl of 1:20 diluted cDNA and a final 0.5µM concentration of
570 each primer (Table 1). Quantification of influenza virus nucleic acid load in
571 tissues was performed in 96-well plates with a 10µL final volume according
572 to the manufacturer's instructions (iTaq SYBR green PCR, BioRad), along
573 with 2µL of cDNA and a final 0.5µM concentration of $H5N8_{HP}$ or $H5N8_{LP}$
574 specific primers. qPCR was performed on a LightCycler 96 (Roche). Relative
575 quantification was carried out by using the $2^{-\Delta Ct}$ method. Chickens: RNA
576 levels were normalized with the geometric mean of GAPDH/HPRT1 mRNA
577 levels. Ducks: mRNA levels were normalized with the geometrics means of
578 RPL4/RPL30 mRNA levels in the lungs and RPL4/GAPDH in the brain.
579 Oropharyngeal Mx mRNA expression was performed in 96-well plates with
580 a final volume of 10µL according to the manufacturer's instructions (iTaq
581 SYBR green one-step, BioRad), with 2µL RNA and a final 0.3µM
582 concentration of each primer. Mx mRNA levels were normalized with
583 GAPDH mRNA levels in chickens and ducks samples using the $2^{-\Delta Ct}$ method.

584

585 **Immunohistochemistry**

586 Tissue samples of the lungs and brain were taken and stored in 10%
587 neutral formalin. After fixation, tissues were processed in paraffin blocks,
588 sectioned at 4µm, and immunohistochemistry was performed on paraffin-
589 embedded sections with a monoclonal mouse anti-nucleoprotein influenza
590 A virus antibody (Argene 11-030; pronase 0.05% retrieval solution, 10 min
591 at 37°C: antibody dilution 1/50, incubation overnight at 4°C). The
592 immunohistochemical staining was revealed with a biotinylated polyclonal
593 goat anti-mouse immunoglobulin conjugated with horseradish peroxidase
594 (HRP; Dako, LSAB2 system-HRP, K0675) and the diaminobenzidine HRP

595 chromogen (Thermo Scientific, TA-125-HDX). Negative controls comprised
596 sections incubated either without specific primary antibody or with
597 another monoclonal antibody of the same isotype (IgG2).
598

599

600 Table 1: Primers used for qPCR

Gene name	Primers sequences (5' to 3')	NCBI accession number or Reference
HA $H5N8_{HP}$	CCCAAACAGCCCTCTTT	
	GGCTCAGAAATAGTCCTCT	
HA $H5N8_{LP}$	GCCATTCATCCACAGTTGACA	
	CATGGTGCTGACAGTGGAGTCT	
HA $H5N8_{LP}$ and $_{HP}$	GACCTCTGTTACCCAGGGAGCCT	
	GGACAAGCTGCGCTTACCCCT	
Chicken HPRT1	TGGTGGGGATGACCTCTCAA	[49]
	GGCCGATATCCCACACTTCG	
Chicken GADPH	TCCTCTCTGGCAAAGTCCAAG	[50]
	CACAACATACTCAGCACCTGC	
Duck GAPDH	CCACTTCCGGGGCACTGTCA	AY436595.1
	AGCACCAGCATCTGCCCACT	
Chicken IFN-γ	ACACTGACAAGTCAAAGCCGC	[51]
	AGTCGTTCATCGGGAGCTTG	
Duck IFN-γ	ACCTCGTGGAACTGTCAAACCT	AF087134
	CAGCTCACTCACAGCCTTGC	
Chicken Mx	CACTGCAACAAGCAAAGAAGGA	[52]
	TGATCAACCCCACAAGGAAAA	
Duck Mx	TCACACGAAGGCCTATTTTACTGG	Z21549
	GTCGCCGAAGTCATGAAGGA	
Duck RPL4	AAGCTGAACCCATACGCCAA	XM_005015528
	CCTGGGCCTTAGCTGTAACC	

Duck RPL30	GCAAAGCCAAGCTGGTCATC	XM_027452502.1
	CTCAATGTTGTTGCCGCTGT	

601 GAPDH, glyceraldehyde-3-phosphate dehydrogenase; HPRT1, hypoxanthine
602 phosphoribosyltransferase 1; IFN-γ, interferon gamma; Mx, Mx Dynamin Like
603 GTPase; RPL4/30, ribosomal protein L4/L30; F, forward; R, reverse
604

605 **REFERENCES**

606

607 1. Lee D-H, Criado MF, Swayne DE. Pathobiological Origins and Evolutionary History of
608 Highly Pathogenic Avian Influenza Viruses. Cold Spring Harb Perspect Med. 2021;11.
609 doi:10.1101/cshperspect.a038679

610 2. EFSA Panel on Animal Health and Welfare (AHAW), More S, Bicout D, Bøtner A,
611 Butterworth A, Calistri P, et al. Avian influenza. EFSA J. 2017;15: e04991.
612 doi:10.2903/j.efsa.2017.4991

613 3. Böttcher-Friebertshäuser E, Garten W, Matrosovich M, Klenk HD. The Hemagglutinin: A
614 Determinant of Pathogenicity. In: Compans RW, Oldstone MBA, editors. Influenza
615 Pathogenesis and Control - Volume I. Cham: Springer International Publishing; 2014.
616 pp. 3–34. doi:10.1007/82_2014_384

617 4. Abdelwhab E-SM, Veits J, Mettenleiter TC. Genetic changes that accompanied shifts of
618 low pathogenic avian influenza viruses toward higher pathogenicity in poultry.
619 Virulence. 2013;4: 441–452. doi:10.4161/viru.25710

620 5. Richard M, Fouchier R, Monne I, Kuiken T. Mechanisms and risk factors for mutation
621 from low to highly pathogenic avian influenza virus. EFSA Supporting Publications.
622 2017;14: 1287E. doi:10.2903/sp.efsa.2017.EN-1287

623 6. McCrone JT, Lauring AS. Genetic bottlenecks in intraspecies virus transmission. Current
624 Opinion in Virology. 2018;28: 20–25. doi:10.1016/j.coviro.2017.10.008

625 7. Hughes J, Allen RC, Baguelin M, Hampson K, Baillie GJ, Elton D, et al. Transmission of
626 Equine Influenza Virus during an Outbreak Is Characterized by Frequent Mixed
627 Infections and Loose Transmission Bottlenecks. PLOS Pathogens. 2012;8: e1003081.
628 doi:10.1371/journal.ppat.1003081

629 8. Varble A, Albrecht RA, Backes S, Crumiller M, Bouvier NM, Sachs D, et al. Influenza A
630 Virus Transmission Bottlenecks Are Defined by Infection Route and Recipient Host. Cell
631 Host & Microbe. 2014;16: 691–700. doi:10.1016/j.chom.2014.09.020

632 9. Bodewes R, Kuiken T. Changing Role of Wild Birds in the Epidemiology of Avian Influenza
633 A Viruses. Adv Virus Res. 2018;100: 279–307. doi:10.1016/bs.aivir.2017.10.007

634 10. Wahlgren J. Influenza A viruses: an ecology review. Infect Ecol Epidemiol. 2011;1.
635 doi:10.3402/iee.v1i0.6004

636 11. Munster VJ, Baas C, Lexmond P, Waldenström J, Wallensten A, Fransson T, et al. Spatial,
637 Temporal, and Species Variation in Prevalence of Influenza A Viruses in Wild Migratory
638 Birds. PLOS Pathog. 2007;3: e61. doi:10.1371/journal.ppat.0030061

639 12. van Dijk JG, Verhagen JH, Wille M, Waldenström J. Host and virus ecology as
640 determinants of influenza A virus transmission in wild birds. Curr Opin Virol. 2018;28:
641 26–36. doi:10.1016/j.coviro.2017.10.006

642 13. Guinat C, Nicolas G, Vergne T, Bronner A, Durand B, Courcoul A, et al. Spatio-temporal
643 patterns of highly pathogenic avian influenza virus subtype H5N8 spread, France, 2016

644 to 2017. Eurosurveillance. 2018;23: 1700791. doi:10.2807/1560-
645 7917.ES.2018.23.26.1700791

646 14. More S, Bicout D, Bøtner A, Butterworth A, Calistri P, Depner K, et al. Urgent request on
647 avian influenza. EFSA Journal. 2017;15: e04687.
648 doi:https://doi.org/10.2903/j.efsa.2016.4687

649 15. Grund C, Hoffmann D, Ulrich R, Naguib M, Schinköthe J, Hoffmann B, et al. A novel
650 European H5N8 influenza A virus has increased virulence in ducks but low zoonotic
651 potential. Emerg Microbes Infect. 2018;7: 132. doi:10.1038/s41426-018-0130-1

652 16. Kleyheeg E, Slaterus R, Bodewes R, Rijks JM, Spierenburg MAH, Beerens N, et al. Deaths
653 among Wild Birds during Highly Pathogenic Avian Influenza A(H5N8) Virus Outbreak,
654 the Netherlands. Emerg Infect Dis. 2017;23: 2050–2054. doi:10.3201/eid2312.171086

655 17. Hiono T, Okamatsu M, Igarashi M, McBride R, de Vries RP, Peng W, et al. Amino acid
656 residues at positions 222 and 227 of the hemagglutinin together with the
657 neuraminidase determine binding of H5 avian influenza viruses to sialyl Lewis X. Arch
658 Virol. 2016;161: 307–316. doi:10.1007/s00705-015-2660-3

659 18. Li S, Bai S, Qin X, Zhang J, Irwin DM, Zhang S, et al. Comparison of whole embryonic
660 development in the duck (Anas platyrhynchos) and goose (Anser cygnoides) with the
661 chicken (Gallus gallus). Poultry Science. 2019;98: 3278–3291. doi:10.3382/ps/pez133

662 19. Leyson C, Youk S-S, Smith D, Dimitrov K, Lee D-H, Larsen LE, et al. Pathogenicity and
663 genomic changes of a 2016 European H5N8 highly pathogenic avian influenza virus
664 (clade 2.3.4.4) in experimentally infected mallards and chickens. Virology. 2019;537:
665 172–185. doi:10.1016/j.virol.2019.08.020

666 20. Holzinger D, Jorns C, Stertz S, Boisson-Dupuis S, Thimme R, Weidmann M, et al.
667 Induction of MxA Gene Expression by Influenza A Virus Requires Type I or Type III
668 Interferon Signaling. Journal of Virology. 2007;81: 7776–7785. doi:10.1128/JVI.00546-
669 06

670 21. Baccam P, Beauchemin C, Macken CA, Hayden FG, Perelson AS. Kinetics of Influenza A
671 Virus Infection in Humans. Journal of Virology. 2006;80: 7590–7599.
672 doi:10.1128/JVI.01623-05

673 22. Soubies SM, Hoffmann TW, Croville G, Larcher T, Ledevin M, Soubieux D, et al. Deletion
674 of the C-terminal ESEV domain of NS1 does not affect the replication of a low-
675 pathogenic avian influenza virus H7N1 in ducks and chickens. J Gen Virol. 2013;94: 50–
676 58. doi:10.1099/vir.0.045153-0

677 23. Volmer C, Soubies SM, Grenier B, Guérin J-L, Volmer R. Immune response in the duck
678 intestine following infection with low-pathogenic avian influenza viruses or stimulation
679 with a Toll-like receptor 7 agonist administered orally. J Gen Virol. 2011;92: 534–543.
680 doi:10.1099/vir.0.026443-0

681 24. Hagenaars TJ, Fischer E a. J, Jansen CA, Rebel JMJ, Spekreijse D, Vervelde L, et al.
682 Modelling the Innate Immune Response against Avian Influenza Virus in Chicken. PLOS
683 ONE. 2016;11: e0157816. doi:10.1371/journal.pone.0157816

684 25. Kumar N, Sharma S, Barua S, Tripathi BN, Rouse BT. Virological and Immunological
685 Outcomes of Coinfections. Clinical Microbiology Reviews. 2018;31.
686 doi:10.1128/CMR.00111-17

687 26. DaPalma T, Doonan BP, Trager NM, Kasman LM. A systematic approach to virus–virus
688 interactions. Virus Research. 2010;149: 1–9. doi:10.1016/j.virusres.2010.01.002

689 27. Opatowski L, Baguelin M, Eggo RM. Influenza interaction with cocirculating pathogens
690 and its impact on surveillance, pathogenesis, and epidemic profile: A key role for
691 mathematical modelling. PLOS Pathogens. 2018;14: e1006770.
692 doi:10.1371/journal.ppat.1006770

693 28. Phipps KL, Ganti K, Jacobs NT, Lee C-Y, Carnaccini S, White MC, et al. Collective
694 interactions augment influenza A virus replication in a host-dependent manner. Nat
695 Microbiol. 2020;5: 1158–1169. doi:10.1038/s41564-020-0749-2

696 29. Andreu-Moreno I, Bou J-V, Sanjuán R. Cooperative nature of viral replication. Sci Adv.
697 2020;6. doi:10.1126/sciadv.abd4942

698 30. Bou J-V, Geller R, Sanjuán R. Membrane-Associated Enteroviruses Undergo Intercellular
699 Transmission as Pools of Sibling Viral Genomes. Cell Rep. 2019;29: 714-723.e4.
700 doi:10.1016/j.celrep.2019.09.014

701 31. Domingo-Calap P, Segredo-Otero E, Durán-Moreno M, Sanjuán R. Social evolution of
702 innate immunity evasion in a virus. Nat Microbiol. 2019;4: 1006–1013.
703 doi:10.1038/s41564-019-0379-8

704 32. Brooke CB. Population Diversity and Collective Interactions during Influenza Virus
705 Infection. Journal of Virology. 2017;91. doi:10.1128/JVI.01164-17

706 33. Kuchipudi SV, Tellabati M, Sebastian S, Londt BZ, Jansen C, Vervelde L, et al. Highly
707 pathogenic avian influenza virus infection in chickens but not ducks is associated with
708 elevated host immune and pro-inflammatory responses. Vet Res. 2014;45: 118.
709 doi:10.1186/s13567-014-0118-3

710 34. Cornelissen JBWJ, Vervelde L, Post J, Rebel JMJ. Differences in highly pathogenic avian
711 influenza viral pathogenesis and associated early inflammatory response in chickens
712 and ducks. Avian Pathol. 2013;42: 347–364. doi:10.1080/03079457.2013.807325

713 35. Cornelissen JBWJ, Post J, Peeters B, Vervelde L, Rebel JMJ. Differential innate responses
714 of chickens and ducks to low-pathogenic avian influenza. Avian Pathol. 2012;41: 519–
715 529. doi:10.1080/03079457.2012.732691

716 36. Burggraaf S, Karpala AJ, Bingham J, Lowther S, Selleck P, Kimpton W, et al. H5N1
717 infection causes rapid mortality and high cytokine levels in chickens compared to
718 ducks. Virus Res. 2014;185: 23–31. doi:10.1016/j.virusres.2014.03.012

719 37. Barber MRW, Aldridge JR, Webster RG, Magor KE. Association of RIG-I with innate
720 immunity of ducks to influenza. Proc Natl Acad Sci USA. 2010;107: 5913–5918.
721 doi:10.1073/pnas.1001755107

722 38. Magor KE, Miranzo Navarro D, Barber MRW, Petkau K, Fleming-Canepa X, Blyth GAD, et
723 al. Defense genes missing from the flight division. Developmental & Comparative
724 Immunology. 2013;41: 377–388. doi:10.1016/j.dci.2013.04.010

725 39. Zwart MP, Elena SF. Matters of Size: Genetic Bottlenecks in Virus Infection and Their
726 Potential Impact on Evolution. Annu Rev Virol. 2015;2: 161–179. doi:10.1146/annurev-
727 virology-100114-055135

728 40. Kuss SK, Etheredge CA, Pfeiffer JK. Multiple host barriers restrict poliovirus trafficking in
729 mice. PLoS Pathog. 2008;4: e1000082. doi:10.1371/journal.ppat.1000082

730 41. Graaf A, Ulrich R, Maksimov P, Scheibner D, Koethe S, Abdelwhab EM, et al. A viral race
731 for primacy: co-infection of a natural pair of low and highly pathogenic H7N7 avian
732 influenza viruses in chickens and embryonated chicken eggs. Emerg Microbes Infect.
733 2018;7: 204. doi:10.1038/s41426-018-0204-0

734 42. Poultry species | Gateway to poultry production and products | Food and Agriculture
735 Organization of the United Nations. [cited 9 Mar 2021]. Available:
736 http://www.fao.org/poultry-production-products/production/poultry-species/en/

737 43. Dhingra MS, Artois J, Dellicour S, Lemey P, Dauphin G, Von Dobschuetz S, et al.
738 Geographical and Historical Patterns in the Emergences of Novel Highly Pathogenic
739 Avian Influenza (HPAI) H5 and H7 Viruses in Poultry. Front Vet Sci. 2018;5.
740 doi:10.3389/fvets.2018.00084

741 44. M.c JD, A S, Der GJV, G K. Intra- and interspecies transmission of H7N7 highly pathogenic
742 avian influenza virus during the avian influenza epidemic in the Netherlands in 2003.
743 2009;28: 333–340. doi:10.20506/rst.28.1.1859

744 45. Capua I, Marangon S. The avian influenza epidemic in Italy, 1999-2000: a review. Avian
745 Pathol. 2000;29: 289–294. doi:10.1080/03079450050118403

746 46. Organization WH. Addressing ethical issues in pandemic influenza planning: discussion
747 papers. World Health Organization; 2008.

748 47. Hoffmann E, Neumann G, Kawaoka Y, Hobom G, Webster RG. A DNA transfection system
749 for generation of influenza A virus from eight plasmids. Proc Natl Acad Sci USA.
750 2000;97: 6108–6113. doi:10.1073/pnas.100133697

751 48. Hoffmann E, Stech J, Guan Y, Webster RG, Perez DR. Universal primer set for the full-
752 length amplification of all influenza A viruses. Arch Virol. 2001;146: 2275–2289.

753 49. Garrido D, Chanteloup NK, Trotereau A, Lion A, Bailleul G, Esnault E, et al.
754 Characterization of the Phospholipid Platelet-Activating Factor As a Mediator of
755 Inflammation in Chickens. Front Vet Sci. 2017;4. doi:10.3389/fvets.2017.00226

756 50. Figueroa T, Boumart I, Coupeau D, Rasschaert D. Hyperediting by ADAR1 of a new
757 herpesvirus lncRNA during the lytic phase of the oncogenic Marek's disease virus.
758 Journal of General Virology,. 2016;97: 2973–2988. doi:10.1099/jgv.0.000606

759 51. Brisbin JT, Gong J, Parvizi P, Sharif S. Effects of lactobacilli on cytokine expression by
760 chicken spleen and cecal tonsil cells. Clin Vaccine Immunol. 2010;17: 1337–1343.
761 doi:10.1128/CVI.00143-10

762 52. James J, Smith N, Ross C, Iqbal M, Goodbourn S, Digard P, et al. The cellular localization
763 of avian influenza virus PB1-F2 protein alters the magnitude of IFN2 promoter and
764 NFκB-dependent promoter antagonism in chicken cells. Journal of General Virology,.
765 2019;100: 414–430. doi:10.1099/jgv.0.001220

766

767

ACKNOWLEDGEMENTS

We thank Jean-Luc Guérin, Marie Souvestre and Luc Robertet (Ecole nationale vétérinaire de Toulouse) for providing clinical samples that enabled the isolation of the A/mulard duck/France/171201g/2017 (H5N8) virus. This work was funded by a grant from the Agence Nationale de la Recherche (ANR-16-CE35-0005-01) to RV. PB was supported by a Ph.D. scholarship funded by the Region Occitanie (France) and by the Chaire de Biosécurité at the École Nationale Vétérinaire de Toulouse (French Ministry of Agriculture). MFB and GD are supported by PhD scholarships funded by the French Ministry of Research and Education.

AUTHOR CONTRIBUTIONS

P.B., T.F. and R.V. conceptualized and designed experiments. P.B., T.F., A.C., C.F.L., A.H., M.F.B., G.D., M.D. and R.V. performed experiments. P.B., T.F. and R.V. analysed data. R.V. acquired funding. P.B. and R.V drafted the manuscript. All authors reviewed and edited the final manuscript before submission.

COMPETING INTERESTS

The authors declare no competing interests.

MATERIALS & CORRESPONDANCE

Correspondence and material requests should be addressed to Romain Volmer (romain.volmer@envt.fr).

791

792 **FIGURES**

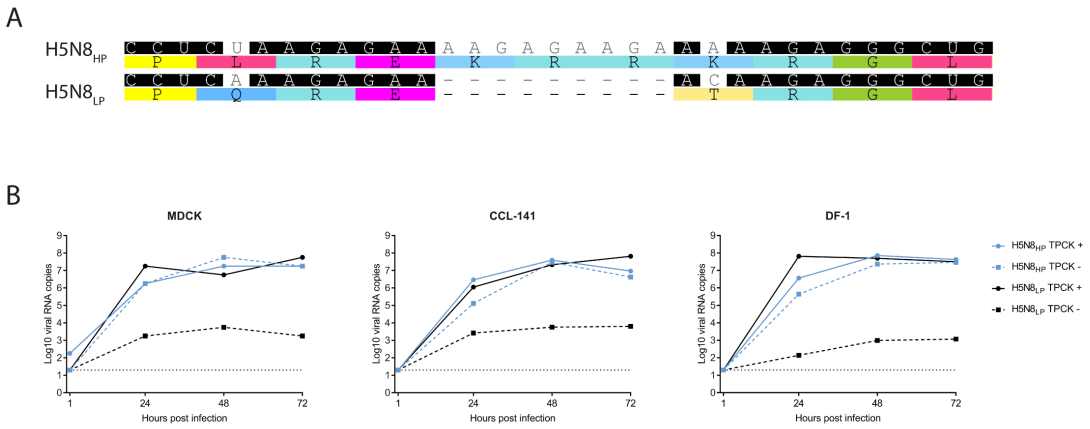

Fig. 1. Characterization of H5N8$_{HP}$ and H5N8$_{LP}$ viruses in cell culture. (A) Sequence alignment of H5N8$_{HP}$ and H5N8$_{LP}$ HA cleavage sites. **(B)** H5N8$_{HP}$ and H5N8$_{LP}$ growth kinetics in the absence or presence of exogenous trypsin in Madin-Darby canine kidney (MDCK) cells, DF-1 cells and CCL-141 cells. Cells were infected at a MOI of 10^{-5} TCID$_{50}$. HA RNA load was analyzed by RT-qPCR using primers common to H5N8$_{HP}$ and H5N8$_{LP}$. The dotted line represents the limit of detection for each experiment. Results are representative of an experiment performed three times.

793

794

A

	H2	L2H2	L3H2	L4H2	L5H2	L2	L3	L4	L5
$H5N8_{HP}$	10^2 EID_{50}	10^2 EID_{50}	10^2 EID_{50}	10^2 EID_{50}	10^4 EID_{50}	-	-	-	-
$H5N8_{LP}$	-	10^2 EID_{50}	10^3 EID_{50}	10^4 EID_{50}	10^5 EID_{50}	10^2 EID_{50}	10^3 EID_{50}	10^4 EID_{50}	10^5 EID_{50}

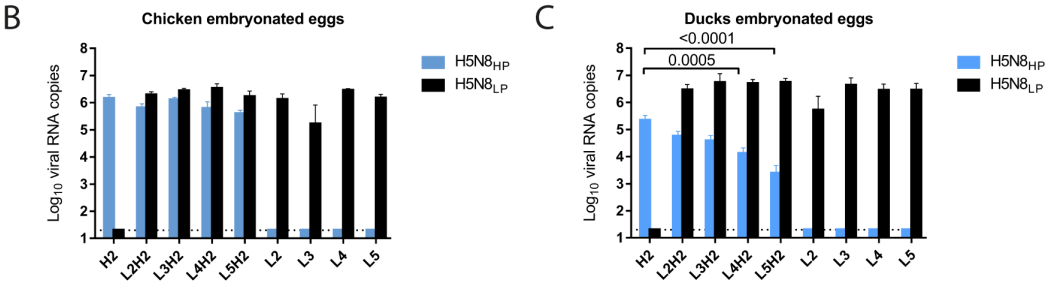

Fig. 2. $H5N8_{HP}$ has a stronger advantage over $H5N8_{LP}$ in embryonated chicken eggs than in embryonated duck eggs. (A) EID_{50} doses used in the *in ovo* experiments**. (B-C)** Chicken **(B)** and duck **(C)** embryonated eggs were infected in the allantoic cavity either with $H5N8_{HP}$ or $H5N8_{LP}$ alone, or with a combination of both. Following a 24 hours incubation at 37°C, viral RNA was extracted from the allantoic fluid and HA levels were determined by RT-qPCR using $H5N8_{HP}$ or $H5N8_{LP}$ specific primers. Statistical analysis: chicken embryonated eggs: n=9 (experiment performed twice); duck embryonated eggs: n=26 (experiment performed three times); one-way ANOVA with Tukey's multiple comparisons test. Results are expressed as means ± SEM. The dotted line represents the limit of detection for each experiment.

795

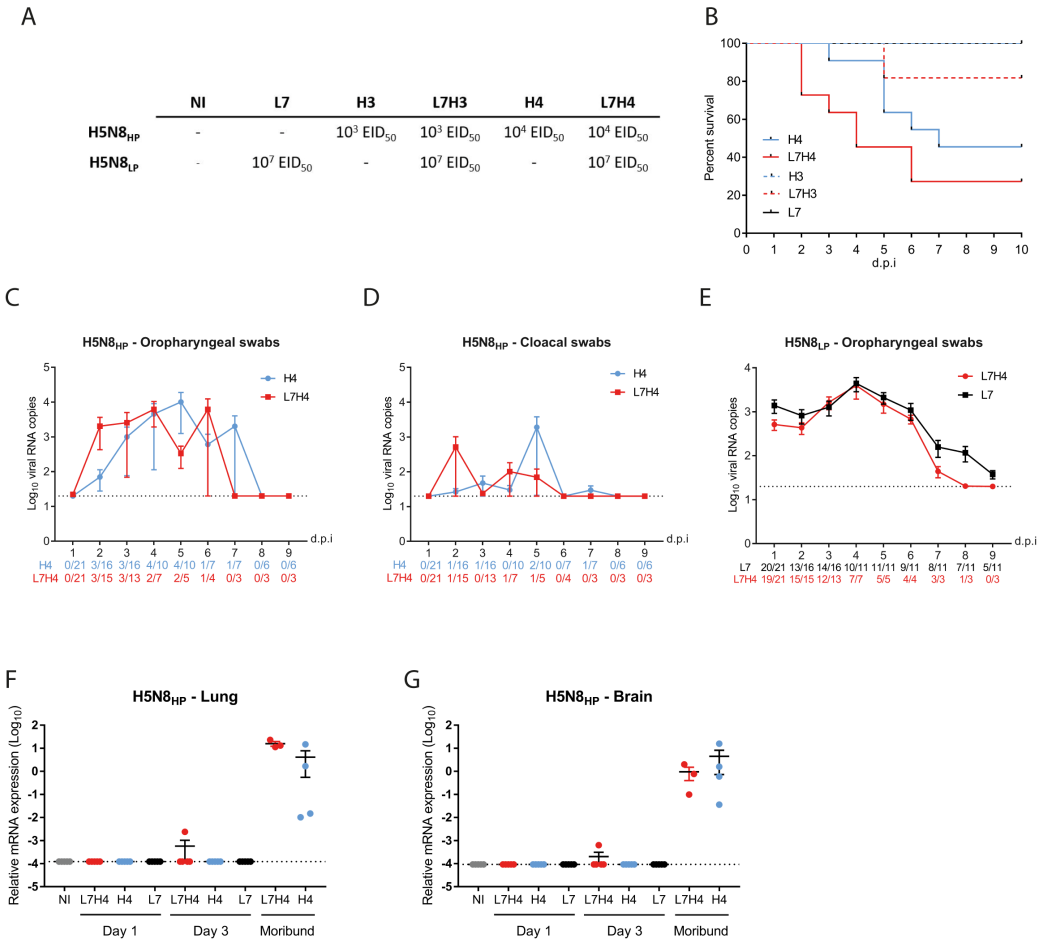

Fig. 3. H5N8$_{HP}$ and H5N8$_{LP}$ coinfection in chickens results in increased pathogenesis. Chickens were inoculated via the choanal route with H5N8$_{LP}$ alone (L7), H5N8$_{HP}$ alone (H3 and H4) or with a combination of H5N8$_{LP}$ and H5N8$_{HP}$ (L7H3 and L7H4). **(A)** EID$_{50}$ doses used in the *in vivo* chicken experiments**. (B)** Survival curves. Statistical analysis: Log-rank (Mantel-Cox) test. **(C-E)** Viral shedding was analyzed by quantifying HA RNA levels by RT-qPCR using H5N8$_{HP}$ specific primers from RNA extracted from oropharyngeal swabs **(C)** and cloacal swabs **(D)** or by RT-qPCR using H5N8$_{LP}$ specific primers from RNA extracted from oropharyngeal swabs **(E)**. Numbers of H5N8$_{HP}$ or H5N8$_{HP}$ swab-positive animals are indicated below each time point. Statistical analysis: two-tailed Mann-Whitney test. Results are expressed as means ± SEM. The dotted line represents the limit of detection. **(F-G)** H5N8$_{HP}$ load was analyzed from total RNA extracted from the lungs **(F)** and the brain **(G)** using H5N8$_{HP}$ specific primers. HA RNA levels were normalized using the $2^{-\Delta Ct}$ method. Statistical analysis:

one-way ANOVA with Tukey's multiple comparisons test. Results are expressed as means ± SEM. The dotted line represents the limit of detection. dpi, days post-infection.

796

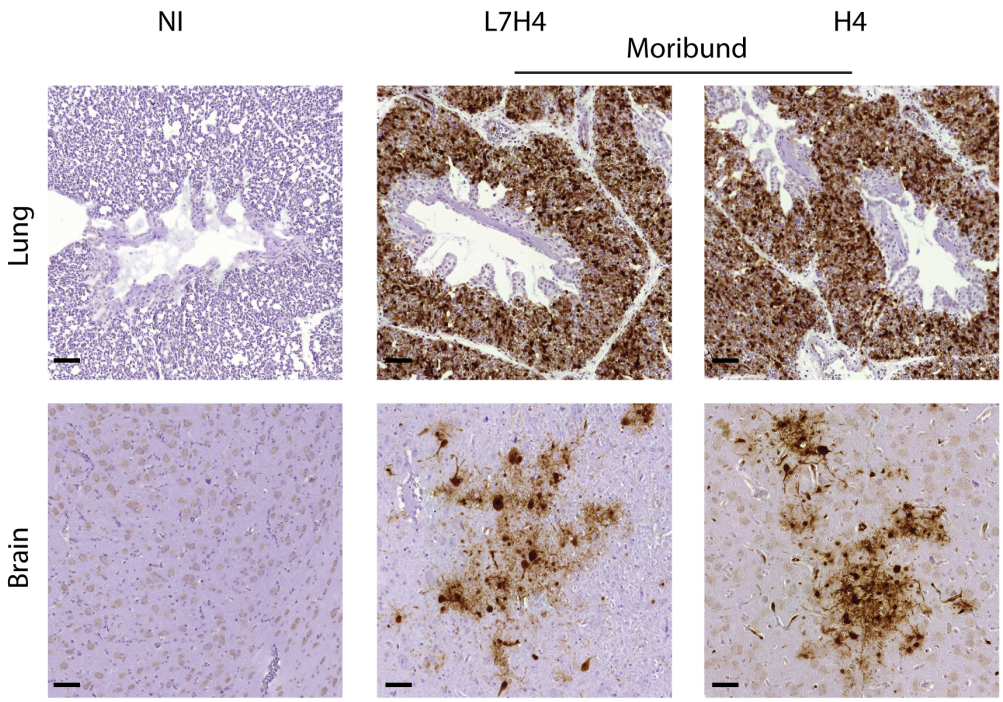

Fig. 4. Immunohistochemical anti-NP staining of hematoxylin-counterstained chickens lung or brain sections. Analysis was performed on non-infected (NI) and moribund chickens. Scale bar, 50 µm.

797

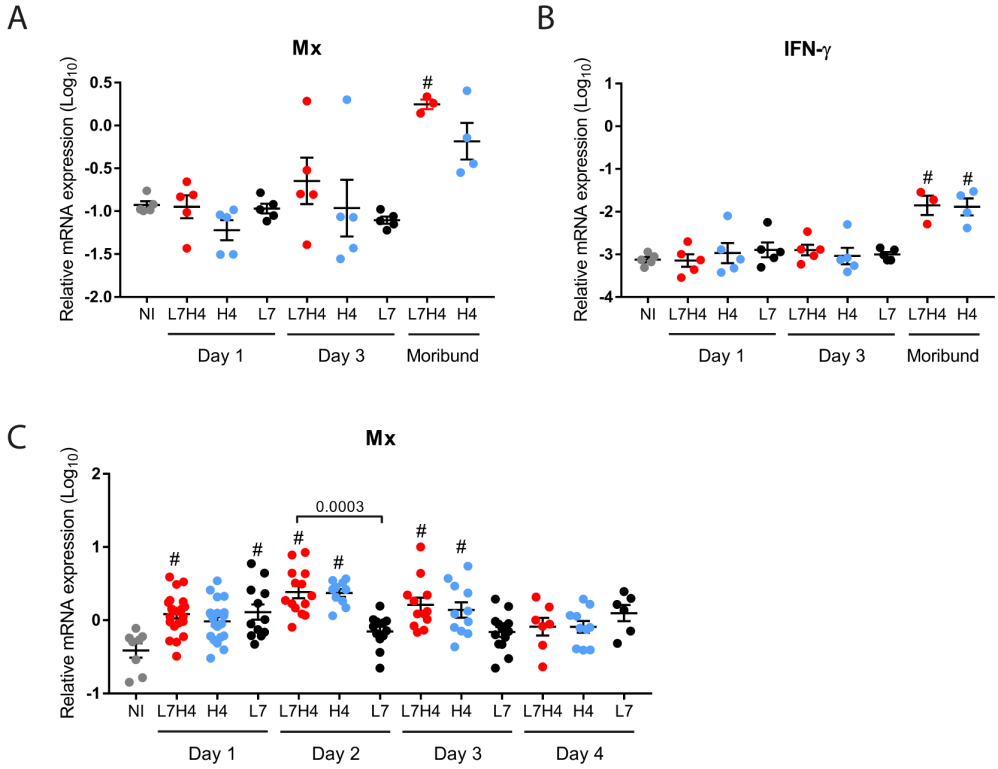

Fig. 5. Mx and IFN-γ mRNA expression following chickens infection. (A-B) mRNA expression levels of Mx **(A)** and IFN-γ **(B)** determined by RT-qPCR performed on lung total RNA. **(C)** mRNA expression levels of Mx determined by RT-qPCR performed on RNA extracted from oropharyngeal swabs. mRNA levels were normalized using the $2^{-\Delta Ct}$ method. Statistical analysis: one-way ANOVA with Tukey's multiple comparisons test. Results are expressed as means ± SEM. #, $p < 0.05$ compared to non-infected (NI) animals.

798

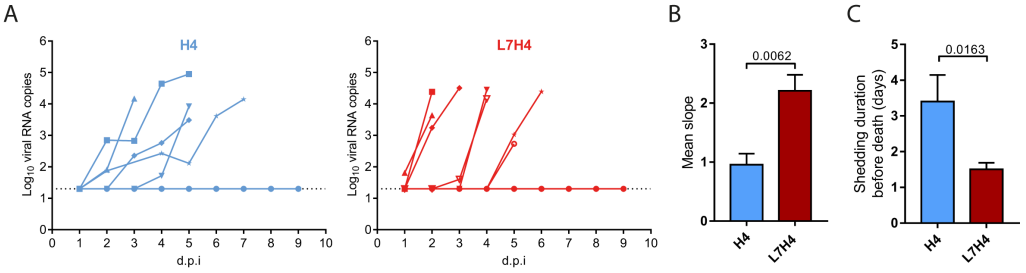

Fig. 6. H5N8$_{HP}$ and H5N8$_{LP}$ coinfection in chickens results in higher H5N8$_{HP}$ growth. (A) Individual H5N8$_{HP}$ oropharyngeal shedding curves in H4 chickens (blue lines) and L7H4 chickens (red lines). Each curve corresponds to a single animal from the onset of H5N8$_{HP}$ excretion to death. **(B)** The slopes of individual H5N8$_{HP}$ excretion curves were calculated. **(C)** H5N8$_{HP}$ shedding duration: number of days where chickens were H5N8$_{HP}$ oropharyngeal swab-positive. Statistical analysis: two-tailed Mann-Whitney test. Results are expressed as means ± SEM. The dotted line corresponds to the limit of detection. dpi, days post-infection.

799

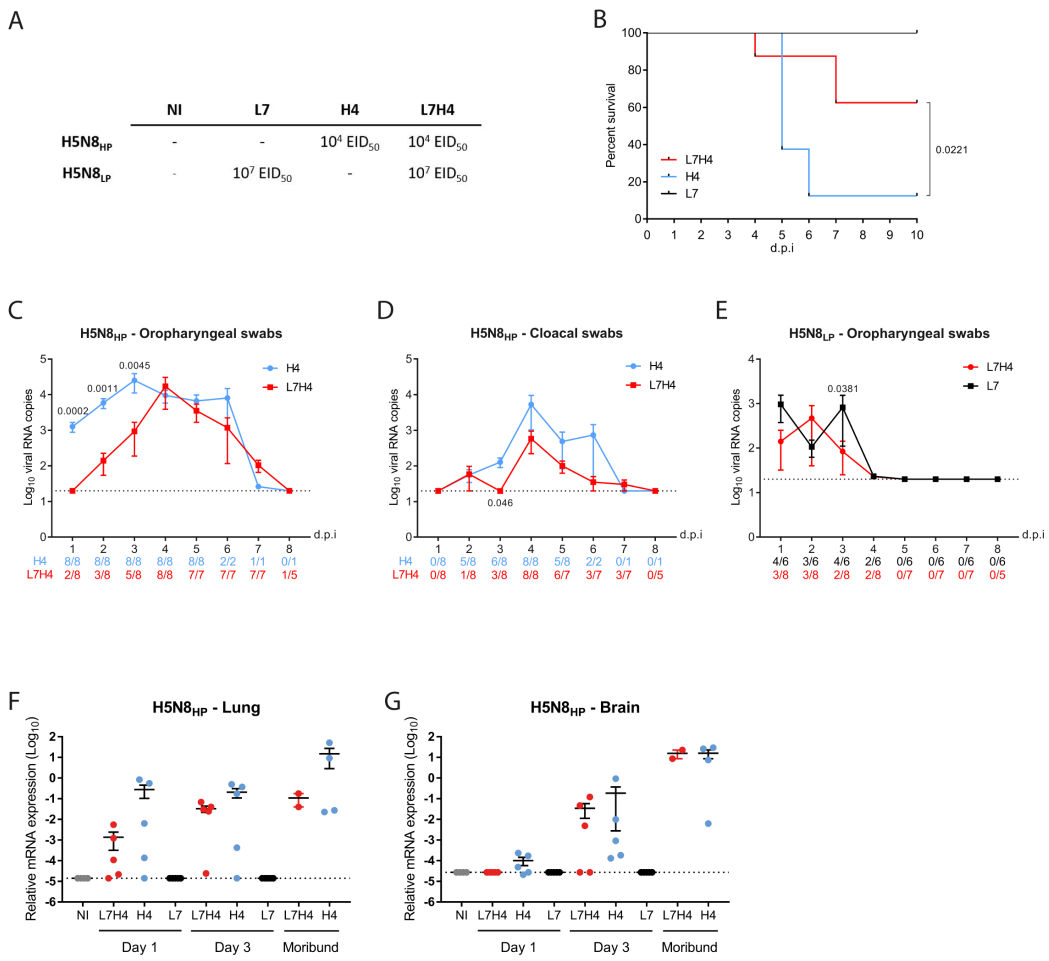

Fig. 7. H5N8$_{HP}$ and H5N8$_{LP}$ coinfection in ducks results in decreased pathogenesis. Ducks were inoculated via the choanal route with H5N8$_{LP}$ alone (L7), H5N8$_{HP}$ alone (H4) or with a combination of H5N8$_{LP}$ and H5N8$_{HP}$ (L7H4). **(A)** EID$_{50}$ doses used in the *in vivo* duck experiments**. (B)** Survival curves. Statistical analysis: Log-rank (Mantel-Cox) test. **(C-E)** Viral shedding was analyzed by quantifying HA RNA levels by RT-qPCR using H5N8$_{HP}$ specific primers from RNA extracted from oropharyngeal swabs **(C)** and cloacal swabs **(D)** or by RT-qPCR using H5N8$_{LP}$ specific primers from RNA extracted from oropharyngeal swabs **(E)**. Numbers of H5N8$_{HP}$ or H5N8$_{HP}$ swab-positive animals are indicated below each time point. Statistical analysis: two-tailed Mann-Whitney test. Results are expressed as means ± SEM. The dotted line represents the limit of detection. **(F-G)** H5N8$_{HP}$ load was analyzed from total RNA extracted from the lungs **(F)** and the brain **(G)** using H5N8$_{HP}$ specific primers. HA RNA levels were

normalized using the $2^{-\Delta Ct}$ method. Statistical analysis: one-way ANOVA with Tukey's multiple comparisons test. Results are expressed as means ± SEM. The dotted line represents the limit of detection. dpi, days post-infection.

800

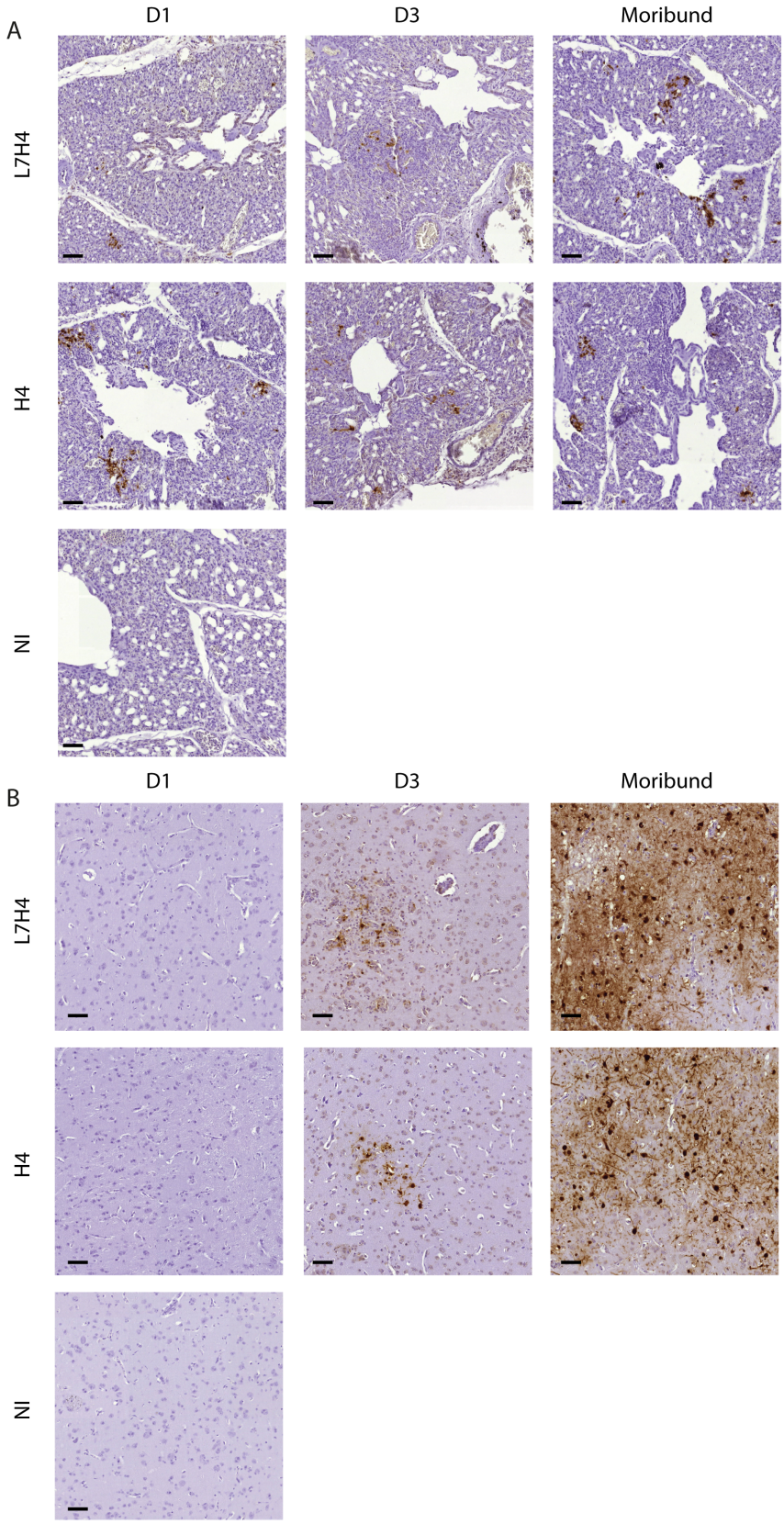

Fig. 8. Immunohistochemical anti-NP staining of hematoxylin-counterstained ducks lung or brain sections. Analysis was performed on

ducks necropsied at 1 (D1) and 3 days (D3) post infection, moribund ducks and non-infected (NI) ducks. **(A)** Lung**. (B)** Brain. Scale bar, 50 μm.

801

802

803

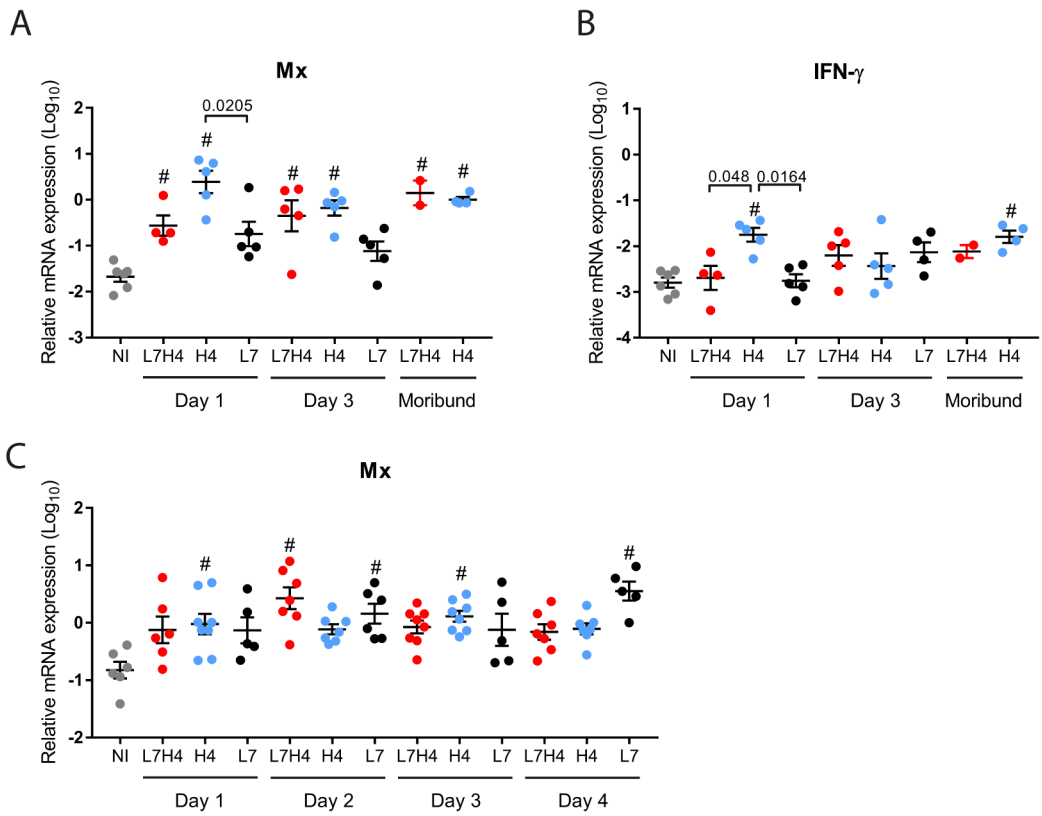

Fig. 9. Mx and IFN-γ mRNA expression following infection in ducks. (A-B) mRNA expression levels of Mx **(A)** and IFN-γ **(B)** determined by RT-qPCR performed on lung total RNA. **(C)** mRNA expression levels of Mx determined by RT-qPCR performed on RNA extracted from oropharyngeal swabs. mRNA levels were normalized using the $2^{-\Delta Ct}$ method. Statistical analysis: one-way ANOVA with Tukey's multiple comparisons test. Results are expressed as means ± SEM. #, $p < 0.05$ compared to non-infected (NI) animals.

804

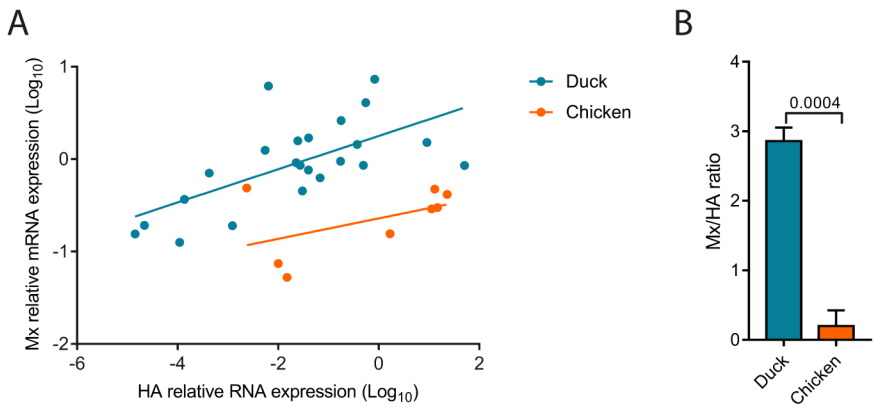

Fig. 10. Ducks mount a more potent antiviral innate immune response compared to chickens. (A) Correlation between Mx mRNA levels and viral RNA levels in the lungs. **(B)** Mean Mx/HA ratios. Mx mRNA and HA RNA levels were normalized using the $2^{-\Delta Ct}$ method. Statistical analysis: two-tailed Mann-Whitney test. Results are expressed as means ± SEM.

805